A VENTILATION INDEX FOR TROPICAL CYCLONES

BY BRIAN TANG AND KERRY EMANUEL

Ventilation—the flux of cooler, drier air into a tropical cyclone—has a pronounced influence on the observed statistics of tropical cyclogenesis and tropical cyclone intensification.

A number of environmental factors control both tropical cyclogenesis and tropical cyclone (TC) intensity, contributing to the challenge of TC prediction. Among these environmental controls is the interaction of TCs with environmental vertical wind shear. Since environmental vertical wind shear is always present in varying amounts during the life of any TC, it is important to understand how wind shear affects TCs to improve genesis and intensity forecasts.

AFFILIATIONS: TANG*—National Center for Atmospheric Research,+ Boulder, Colorado; EMANUEL—Program in Atmospheres, Oceans, and Climate, Massachusetts Institute of Technology, Cambridge, Massachusetts
***CURRENT AFFILIATION:** Department of Atmospheric and Environmental Sciences, University at Albany, State University of New York, Albany, New York
CORRESPONDING AUTHOR: Brian Tang, ES 324, 1400 Washington Ave., Albany, NY 12222
E-mail: btang@albany.edu

+The National Center for Atmospheric Research is sponsored by the National Science Foundation.

The abstract for this article can be found in this issue, following the table of contents.
DOI:10.1175/BAMS-D-11-00165.1

A supplement to this article is available online (10.1175/BAMS-D-11-00165.2)

In final form 11 May 2012

Environmental vertical wind shear is observed to be generally detrimental to tropical cyclogenesis (McBride and Zehr 1981; Zehr 1992), making wind shear an important component of empirical genesis indices (Gray 1979; DeMaria et al. 2001; Emanuel and Nolan 2004). In addition to observations, numerical modeling studies find that sufficiently strong vertical wind shear impedes the development of incipient vortices (Tory et al. 2007; Nolan and Rappin 2008). However, weak shear may aid genesis by forcing synoptic-scale ascent, especially in baroclinic environments (Bracken and Bosart 2000; Davis and Bosart 2006; Nolan and McGauley 2012).

Vertical wind shear may discourage genesis by ventilating the incipient disturbance with low-entropy (low-equivalent potential temperature) air (Simpson and Riehl 1958). Gray (1968) hypothesized that advection by the environmental flow removes the "condensation heat" from a vortex, preventing it from deepening. The environmental flow also advects dry air into the disturbance, disrupting the formation of a deep, moist column that is postulated to be imperative for genesis (Emanuel 1989; Bister and Emanuel 1997; Nolan 2007).

In addition to tropical cyclogenesis, environmental vertical wind shear generally impedes TC intensification. Vertical wind shear is strongly and negatively correlated with intensity changes at various time intervals (DeMaria 1996; Gallina and Velden 2002) and reduces the maximum intensity that a TC can achieve (Rappaport et al. 2010). Thus, vertical

wind shear is one of the most important predictors in statistical–dynamical intensity models (Emanuel et al. 2004; DeMaria et al. 2005; DeMaria 2009). A number of 3D numerical modeling studies of TCs in sheared environments also simulate decreases in intensity, but there are a number of hypotheses as to what causes the weakening. Some hypotheses include outward eddy fluxes of entropy and potential vorticity that erode the TC from the top down (Frank and Ritchie 2001), stabilization caused by midlevel warming (DeMaria 1996), reversal of the secondary circulation on the upshear side allowing entrainment of environmental air at upper levels (Wong and Chan 2004), and eddy momentum fluxes that weaken the mean tangential winds (Wu and Braun 2004).

Another hypothesis is that vertical wind shear acts to decrease the efficiency of the hurricane heat engine by ventilating the TC with low-entropy air at midlevels (Simpson and Riehl 1958; Cram et al. 2007; Marin et al. 2009). Convective downdrafts due to evaporative cooling flush the low-entropy air into the boundary layer, where it is then advected inward by the radial inflow (Powell 1990; Riemer et al. 2010; Riemer and Montgomery 2011). Figure 1 illustrates the ventilation process in a sheared TC.

Tang and Emanuel (2010, hereafter TE10) developed a simple framework to study the constraint of ventilation on TC intensity. Ventilation weakens the TC because it siphons energy away from the TC that would otherwise to be used to power the winds against frictional dissipation. Thus, ventilation acts as an "anti-fuel."

Therefore, ventilation is hypothesized to be an important mechanism by which environmental vertical wind shear controls both tropical cyclogenesis and TC intensification. To provide evidence for this hypothesis, we introduce a ventilation index and provide a qualitative interpretation of its form. Afterward, we use the ventilation index to assess the degree to which ventilation controls global TC genesis and intensity statistics. Finally, we explore some operational applications of the ventilation index.

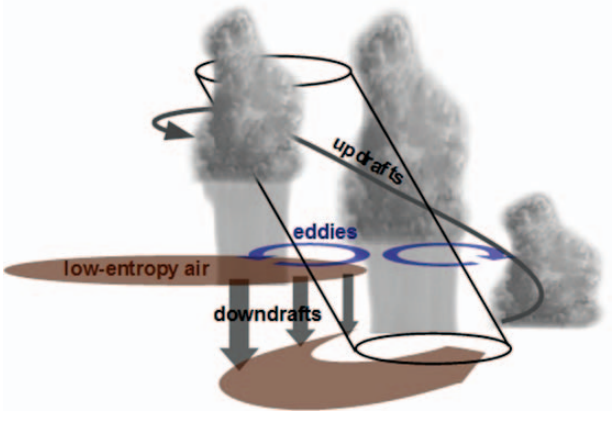

Fig. 1. An illustration of a tropical cyclone undergoing ventilation. The vertically sheared environmental flow tilts the vortex inner core and causes convective asymmetries, which both excite mesoscale eddies. These eddies transport low-entropy air, found at midlevels of the environment, into the TC. The low-entropy air then mixes into the inner core and undercuts helical updrafts, where evaporation of rain produces downdrafts that flush the inflow layer with low-entropy air. These processes counteract the generation of available potential energy by surface fluxes and weaken the TC. Figure adapted from Michael Riemer with permission.

VENTILATION INDEX. The ventilation index, Λ, is defined as

$$\Lambda = \frac{u_{shear}\chi_m}{u_{PI}}, \tag{1}$$

where $u_{shear} = |\mathbf{u}_{850} - \mathbf{u}_{200}|$ is the bulk environmental vertical wind shear between 850 and 200 hPa,[1] χ_m is the (nondimensional) entropy deficit, and u_{PI} is the potential intensity. A derivation of the ventilation index starting from the results of TE10 and details on how to calculate the ventilation index from gridded data can be found in the supplement (available online at http://dx.doi.org/10.1175/BAMS-D-11-00165.2).

The entropy deficit is defined as

$$\chi_m = \frac{s_m^* - s_m}{s_{SST}^* - s_b}, \tag{2}$$

where s_m^* is the saturation entropy at 600 hPa in the inner core of the TC, s_m is the environmental entropy at 600 hPa, s_{SST}^* is the saturation entropy at the sea surface temperature, and s_b is the entropy of the boundary layer. The numerator of (2) is the difference in entropy between the TC and the environment at midlevels, while the denominator is the air–sea disequilibrium. The denominator is evaluated at the radius of maximum wind for a TC at its potential intensity.

For the entropy deficit calculation, the pseudoadiabatic entropy from Bryan (2008) is used:

$$s = c_p \log(T) - R_d \log(p_d) + \frac{L_{vo} r_v}{T} - R_v r_v \log(H), \tag{3}$$

[1] This vertical wind shear metric captures the deep layer shear and may not necessarily reflect the full vertical structure of the environmental winds. Still, this metric does a good job statistically in empirical TC studies (e.g. DeMaria 1996).

where c_p is the specific heat at constant pressure for dry air, T is the temperature, R_d is the gas constant for dry air, p_d is the partial pressure of dry air, L_{vo} is the latent heat of vaporization, r_v is the water vapor mixing ratio, R_v is the gas constant for water vapor, and H is the relative humidity. Note that L_{vo} is set at 2.555×10^6 J kg^{-1} to compensate for neglecting the entropy of water vapor.

The potential intensity of a TC is a theoretical upper bound on the maximum wind speed considering the local thermodynamic profile and gradient wind balance. The potential intensity is calculated using the algorithm from Bister and Emanuel (2002) under pseudoadiabatic assumptions.

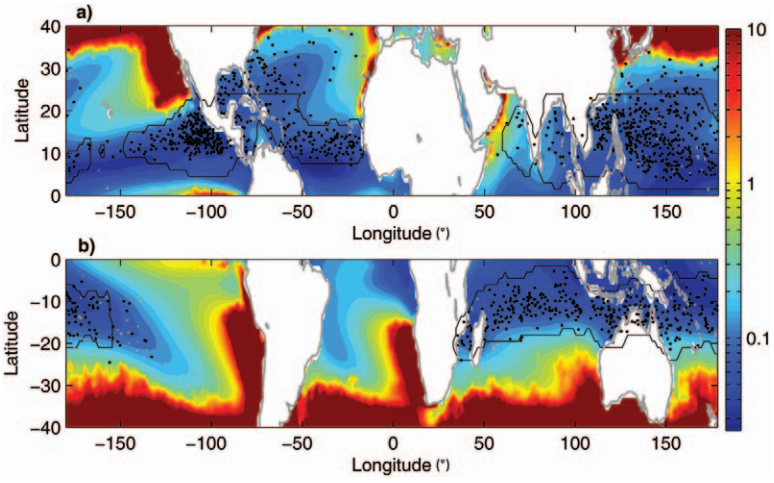

Fig. 2. (a) July–October ventilation index for the Northern Hemisphere and (b) December–March ventilation index for the Southern Hemisphere averaged over 1990–2009. Note the logarithmic scale. Black dots are tropical cyclogenesis points over the same period. Black outline demarcates main genesis regions, which are constrained to be equatorward of 25°.

In essence, it is the combination of the environmental vertical wind shear, the entropy deficit, and the potential intensity that is important to TCs in this ventilation framework. Environmental wind shear tilts the TC and causes structural asymmetries. A cooler and/or drier environment relative to the TC results in a greater entropy deficit, especially if the air–sea disequilibrium (potential intensity) is small. The structural changes induced by the shear together with the entropy deficit combine to allow low-entropy air to intrude into the high-entropy reservoir of the inner core. The intrusion partially negates the energy supplied by surface fluxes, inhibiting the hurricane heat engine by destroying available potential energy and frustrating its conversion to mechanical energy. However, greater surface fluxes (potential intensity) can buffer against the debilitating effects of ventilation by counteracting the intrusion of low-entropy air.

If the wind shear and/or entropy deficit vanishes, the ventilation index vanishes as well. In this case, the hurricane heat engine outputs the maximum work possible, and the TC achieves its potential intensity in this framework. Increasing the ventilation index increases the contribution of the anti-fuel terms compared to surface fluxes, which decreases the work that can be accomplished. As a result, the intensity decreases below its potential intensity. If the ventilation becomes so strong that it overwhelms the surface fluxes, then the TC cannot be sustained and decays.

VENTILATION CLIMATOLOGY. The seasonally averaged (1990–2009) ventilation index is calculated from interim European Centre for Medium-Range Weather Forecasts (ECMWF) Re-Analysis (ERA-Interim) data (Dee et al. 2011). The season is defined as peak four months of each hemisphere's TC season (July–October for the Northern Hemisphere and December–March in the Southern Hemisphere). To resolve detail in the tropics, the results in Fig. 2 are shown on a logarithmic scale. In tropical regions frequented by tropical cyclones, the seasonally averaged ventilation index is less than 0.1. This threshold demarcates regions of relatively high potential intensity (>80 m s^{-1}), low vertical wind shear (<15 m s^{-1}), and low entropy deficit (<0.7). In the subtropics on the eastern side of the ocean basins, relatively low potential intensity, high vertical wind shear, and high entropy deficit coincide to produce tongues of high ventilation. The high entropy deficit in these regions is caused by an abundance of dry air at midlevels. Poleward of 30°, the ventilation increases quickly due to increasing upper-level westerlies and a sharp decrease in potential intensity.

Genesis. Tropical cyclogenesis events, defined as the first appearance of a TC in the National Hurricane Center or Joint Typhoon Warning Center best-track databases, are clearly confined to regions of low seasonal ventilation, as seen in Fig. 2. A notable exception to this pattern is near the equator where there is a dearth of genesis events due to the low Coriolis parameter. Regions where the seasonal ventilation index exceeds 0.3 only have isolated genesis events. Even in the deep tropics, local maxima in the

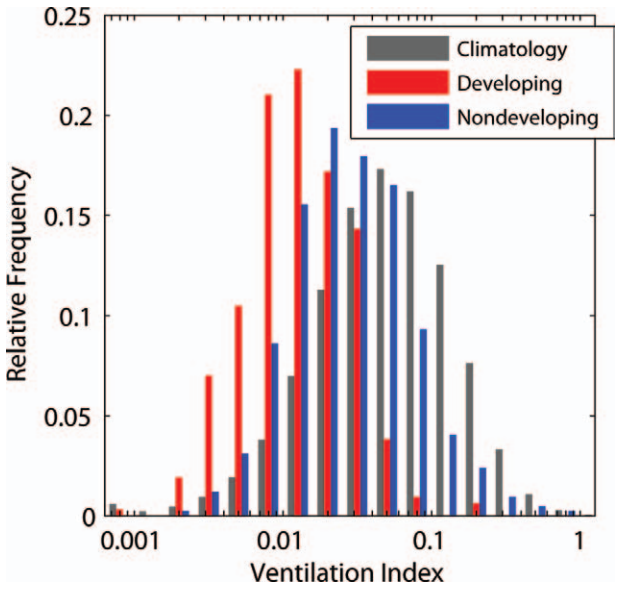

Fig. 3. Normalized ventilation index histograms for the main genesis regions during each hemisphere's tropical cyclone season (gray), developing tropical disturbances (red), and nondeveloping tropical disturbances (blue).

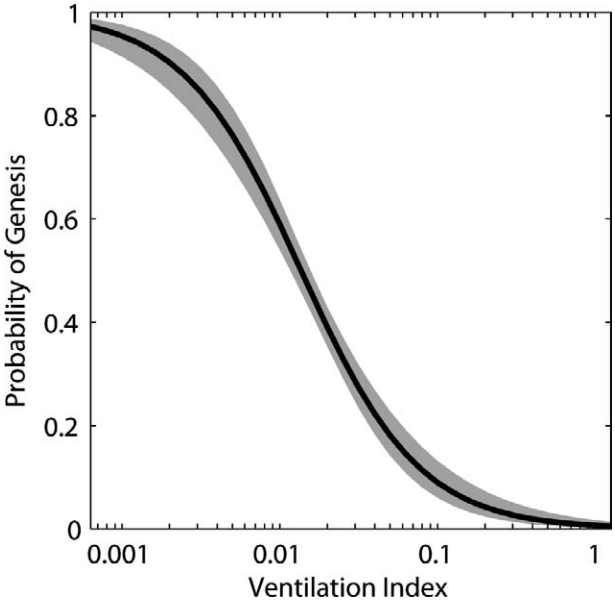

Fig. 4. The probability of genesis as a function of the mean ventilation index over the lifetime of a tropical disturbance, using a logistic regression model. The gray shading gives the 95% confidence interval for the probability of genesis.

ventilation index coincide with minima in the genesis density, such as in the central Caribbean Sea and the western Arabian Sea.

In order to assess the effect of ventilation on individual tropical disturbances, the instantaneous ventilation is calculated following each disturbance. Tropical disturbance tracks are compiled from the National Hurricane Center and Joint Typhoon Warning Center "invest"[2] fixes equatorward of 30° from 2005 to 2009.

Two ventilation index distributions are created. The first distribution comprises developing systems, which are invests that eventually become TCs. The ventilation index for developing systems is averaged over the 24-h period prior to genesis, following the disturbance. The second distribution comprises nondeveloping systems, which are invests that fail to undergo genesis. The ventilation index for nondeveloping systems is averaged over the 24-h period prior to the last record.

Figure 3 shows the ventilation index distributions for both developing and nondeveloping systems along with the climatological ventilation index distribution over the main genesis regions, which are outlined in Fig. 2. Clearly, developing storms preferentially form when the ventilation index is small in the 24 h leading up to genesis. Nondeveloping storms are embedded in environments with higher ventilation indices compared to their developing counterparts but lower than the seasonal climatological background in the main genesis regions. All three distributions in Fig. 3 are significantly different from each other at the 99% level using a Wilcoxon rank sum test.[3]

All three components of the ventilation index contribute to differences in the distributions between developing and nondeveloping disturbances. Compared to nondeveloping disturbances, developing disturbances are found in environments with low to moderate vertical wind shear, higher potential intensities, and lower entropy deficits (moister midlevels). Midlevel moisture is most responsible for the differences between developing and nondeveloping disturbances (not shown). This finding is consistent with the hypothesis that saturating a deep layer of the troposphere is a necessary condition for tropical cyclogenesis.

The genesis probability of a disturbance as a function of the mean ventilation index over the lifetime of the disturbance is quantified using a logistic

[2] Invest areas, as defined by the National Hurricane Center, are "weather systems for which a tropical cyclone forecast center is interested in collecting specialized data sets and/or running model guidance."

[3] The Wilcoxon rank sum test is the nonparametric alternative to the *t* test. A nonparametric test must be used because the distributions are not normal (in linear space).

regression model, as shown in Fig. 4. The probability of genesis is greater than 90% when the mean ventilation index is less than 0.002, 50% when the mean ventilation index is 0.014, and less than 10% when the mean ventilation index is greater than 0.1. In terms of the odds, defined as the probability of genesis divided by one minus the probability of genesis, a 0.1 decrease in $\log_{10}(\Lambda)$ over the lifetime of a disturbance increases the odds of genesis by 31%. Thus, the probability or odds of genesis is strongly dependent on the mean ventilation index of the disturbance, and such probabilities may serve as useful forecast guidance.

Instead of the mean ventilation index, Fig. 5 shows the temporal evolution of the instantaneous ventilation index for developing cases composited before the time of genesis. There is a tendency for the first quartile, median, and third quartile of the ventilation index to decrease as genesis approaches. The sharpest decrease occurs between 96 and 54 h before genesis with only slight decreases thereafter. Between 54 h and genesis, low ventilation indices support an incubation period that allows convection to organize and the circulation to spin up (Raymond and Sessions 2007; Dunkerton et al. 2009).

The ventilation index shares similarities with other empirically derived genesis indices combining dynamical and thermodynamical ingredients that favor genesis. For example, Emanuel (2010) proposed the following genesis potential index (GPI):

$$\mathrm{GPI}=\frac{|\eta|^3 \max(u_{\mathrm{PI}}-35,0)^2}{\chi_m^{4/3}(u_{\mathrm{shear}}+25)^4}, \qquad (4)$$

where η is the absolute vorticity. Comparing (1) and (4) reveals that the GPI is proportional to some negative power of the ventilation index, with an empirical best fit using a power between –1 and –2. Hence, a portion of the spatial and temporal variability of tropical cyclogenesis is explained by ventilation. Since the GPI is a purely empirically derived quantity, some theoretical underpinning is gained by its similarity to the ventilation index, which is derived from an idealized, analytical framework (see supplement).

Moreover, the ventilation index is identical to the "incubation parameter" from Rappin et al. (2010). The incubation parameter has a very high correlation to the genesis time in idealized simulations of tropical cyclogenesis. Additionally, there appears to be a threshold incubation parameter that distinguishes developing and nondeveloping cases. In light of these findings, there is now empirical, theoretical, and modeling evidence for the utility of the ventilation index as an important parameter for tropical cyclogenesis.

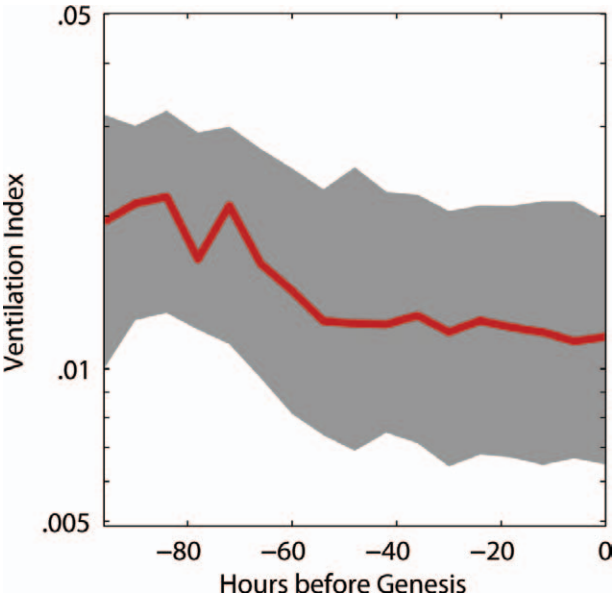

Fig. 5. Ventilation index statistics of developing tropical disturbances composited before the genesis time. The gray shading gives the interquartile range (25th and 75th percentiles), and the red line denotes the median ventilation index.

Intensity. In addition to genesis, ventilation also constrains tropical cyclone intensification. The intensity is given by the 6-hourly near-surface maximum wind speed from the National Hurricane Center and Joint Typhoon Warning Center best-track archives. In order to avoid subtropical storms and extratropical transitioning storms, the data are restricted to storms equatorward of 30°. Additionally, TCs over land are excluded.

It is advantageous to work in a nondimensional framework since the ventilation index itself is nondimensional. Accordingly, the *normalized* intensity of a TC is defined to be the maximum symmetric wind speed divided by the local potential intensity. The maximum symmetric wind speed, u_{sym}, is estimated by using the formula from Schwerdt et al. (1979) to remove the influence of the TC translation speed, c, from the best-track wind speed, u_{BT}:

$$u_{\mathrm{sym}} = u_{\mathrm{BT}} - 1.17c^{0.63}. \qquad (5)$$

Furthermore, before calculating the normalized intensity, the potential intensity is multiplied by 75% to account for the reduction of winds from the top of the boundary layer to the surface in order to conform to the observed data (Franklin et al. 2003).

The *normalized* intensification is defined to be the 24-h change in normalized intensity. It is important to remember that the normalized intensification

differs from the raw intensification since the potential intensity along the TC track changes. For instance, one could have normalized strengthening despite a decrease in actual intensity if the potential intensity along the TC track drops faster than the intensity. Henceforth, the terms "weakening" and "strengthening" will refer to normalized changes in intensity.

The ventilation index for TCs is partitioned in two groups. The first group consists of TCs that strengthen over the subsequent 24 h, while the second group consists of TCs that weaken over the subsequent 24 h. Figure 6 shows the ventilation index distributions for both of these groups. Strengthening TCs tend to have lower ventilation indices than their weakening counterparts. With only a handful of exceptions, an approximate upper bound ventilation index for strengthening TCs is 0.1. The two distributions are significantly different at the 99% level using a Wilcoxon rank sum test.

While there is a significant difference between the ventilation index distributions of strengthening and weakening TCs, it is much more illuminating to examine the normalized intensification distribution as a function of both the ventilation index and the normalized intensity, as shown in Fig. 7a. There is a clear delineation between strengthening and weakening TCs. TCs with low ventilation indices and low-to-intermediate normalized intensities tend to strengthen, while TCs with high ventilation indices and/or high normalized intensities tend to weaken.

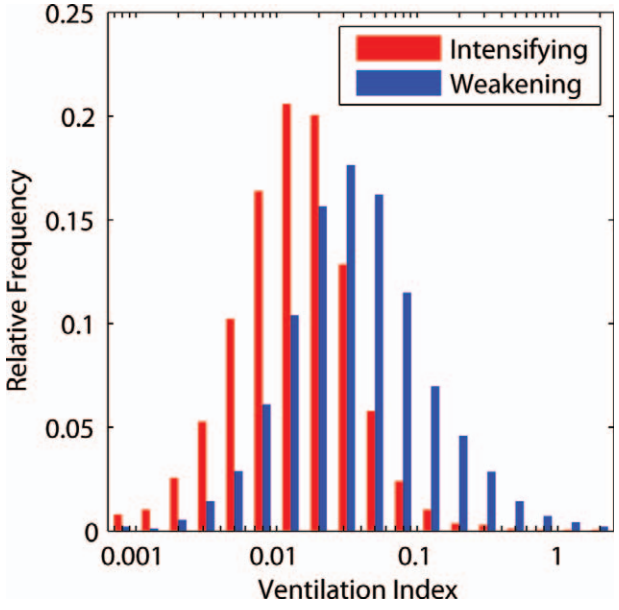

Fig. 6. Normalized ventilation index histograms for intensifying (red) and weakening tropical cyclones (blue).

Additionally, there exists a well-defined boundary separating the two regions, implying an equilibrium boundary to which TCs tend to intensify or weaken. The boundary is approximately horizontal just below the potential intensity, or a normalized intensity of 1.0, for the lowest few ventilation index bins and then bends downward as the ventilation index increases to 0.03. The greatest strengthening tends to occur at low ventilation indices (<0.01) and intermediate normalized intensities (0.2–0.7), while the greatest weakening tends to occur at high ventilation indices (>0.04) and high normalized intensities (>0.5).

The advantage of displaying the normalized intensification in this manner is that it may be compared with the theoretical normalized intensification from TE10. In TE10, there exists a stable equilibrium intensity that describes the balance among surface energy fluxes, frictional dissipation, and ventilation. Greater amounts of ventilation lead to a lower equilibrium intensity. For given amount of ventilation, a TC below its equilibrium intensity intensifies toward it, while a TC above its equilibrium intensity weakens toward it. Mathematical details can be found in the final section of the supplement.

Figure 7b shows the resulting theoretical intensity change as a function of the normalized ventilation[4] and the normalized intensity. It is important to note that the time interval over which the theoretical intensity change occurs is ambiguous in the analytical solution, which prevents direct comparison of the intensification magnitudes with observations. Thus, only the qualitative features of Figs. 7a and 7b may be compared.

With this limitation in mind, there are still some striking similarities between the observed and theoretical intensity changes. The equilibrium boundaries, given by the gray shading where there is no intensification, correspond fairly well for normalized intensities above 0.5. The regions of intensification to the left of the equilibrium boundaries are similar in both, with the core of more rapidly intensifying TCs located in roughly the same region of the phase space. Additionally, there is a high degree of spatial correlation between Figs. 7a and 7b for weakening TCs in the upper half of each figure.

Differences between Figs. 7a and 7b point to where the theory does not capture the intensification behavior well. For instance, the boundary between strengthening and weakening TCs at low normalized

[4] The normalized ventilation scales with the ventilation index. See the supplement for details.

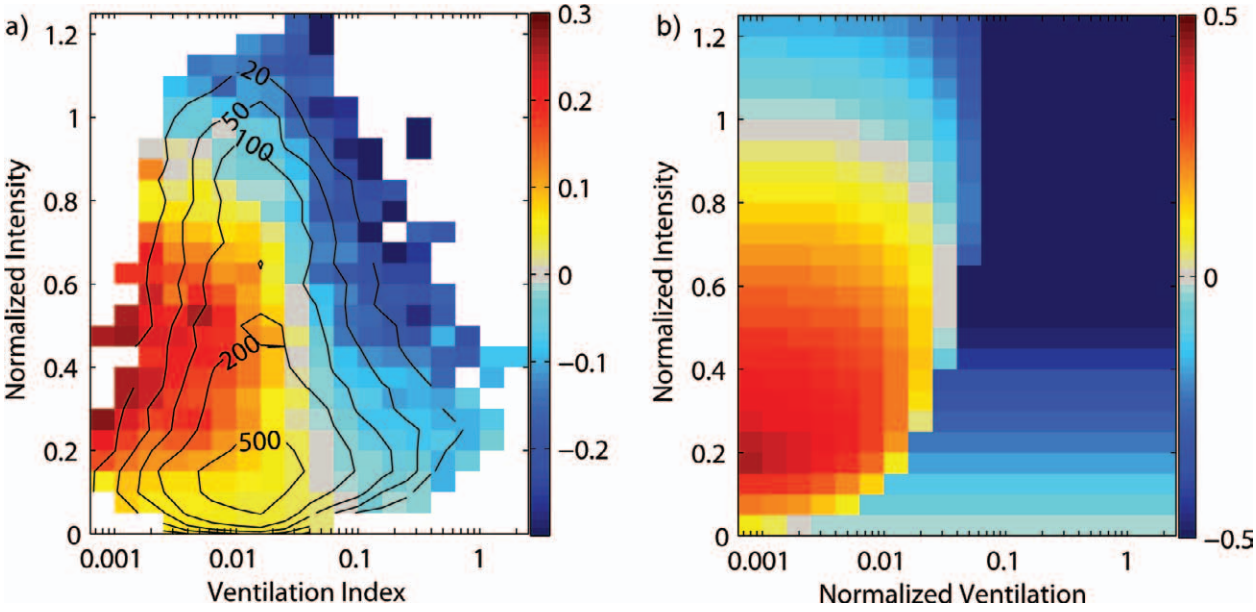

Fig. 7. (a) The observed mean 24-h normalized intensification in each joint ventilation index and normalized intensity bin. The sample size in each bin is contoured. Bins with a sample size less than five are omitted. (b) The theoretical normalized intensification as a function of the normalized ventilation and normalized intensity, as deduced from the analytical framework of TE10 (see supplement for details). The normalized ventilation scales with the ventilation index and has been offset for easier comparison.

intensities (<0.3) is different. The boundary is nearly vertical in observations, but bends back inward toward lower ventilation in the theoretical results. Additionally, the gradient of weakening as the boundary is crossed toward higher values of ventilation is not as stark in observations. A possible explanation for these differences is that for both relatively weak, disorganized storms and highly ventilated, sheared storms, the assumptions used in the theoretical framework—including slantwise neutrality, axisymmetry, and steadiness—do not apply well. The intensification of these types of TCs may be more dependent on transient, mesoscale bursts of convection (Nolan and Montgomery 2002; Molinari et al. 2006; Molinari and Vollaro 2010). This behavior would lead to greater divergence in the intensification statistics from the theory.

Finally, the climatology of rapidly intensifying and weakening storms is examined using the same framework. Kaplan and DeMaria (2003) noted that TCs that rapidly intensify start at intensities well below their potential intensities. Furthermore, they found that rapidly intensifying TCs are embedded in environments with lower shear, higher moisture, and warmer sea surface temperatures compared to TCs that do not undergo rapid intensification. In this study, the threshold for rapid intensification is set at an intensification of 0.2, which for example corresponds to a 15 m s^{-1} increase in maximum winds over a 24-h period in an environment with a constant potential intensity of 75 m s^{-1}.

Figure 8a shows the fraction of TCs undergoing rapid intensification in each joint ventilation index–normalized intensity bin. There is a broad zone where >30% of the TCs undergo rapid intensification. This "danger zone" is roughly bounded by a ventilation index of 0.01 on the right, a normalized intensity of 0.2 on the bottom, and a normalized intensity of 0.7 on the top. For extremely low ventilation indices (<0.002) within this region, the majority of TCs undergo rapid intensification.

Similarly, Fig. 8b shows the fraction of storms undergoing rapid weakening (i.e., TCs that are observed to weaken by at least -0.2). Rapidly weakening storms are located in the upper-right portion of the phase space at normalized intensities greater than 0.4 and ventilation indices generally above 0.04 for TCs below their potential intensity. The high probability of rapid weakening as the normalized intensity and ventilation index both increase to large values weighs against observing large numbers of TCs in this region of the phase space.

OPERATIONAL APPLICATIONS. Since ventilation appears to control the intensification statistics of TCs to a significant degree, ventilation diagnostics are developed in order to assess intensity changes in individual TCs in retrospect and in real time. For

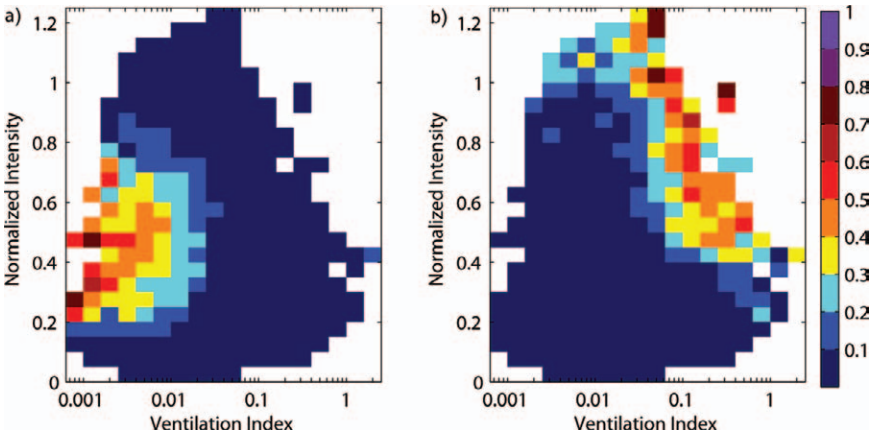

Fig. 8. The fraction of TCs in each joint ventilation index and normalized intensity bin undergoing (a) rapid intensification and (b) rapid weakening, defined as a change in normalized intensity of at least ±0.2 over 24 h.

purposes of demonstration for a retrospective case, Hurricane Felicia from the 2009 eastern North Pacific season is chosen. Felicia is an example of a hurricane that went through a complete life cycle, stayed at relatively low latitudes, and moved at a steady clip, and whose intensity evolution was largely controlled by ventilation. These factors make Felicia a textbook case for ventilation.

Figure 9a shows the track and intensity of Felicia. Felicia underwent genesis at 1800 UTC 3 August 2009, then moved toward the west-northwest and northwest over the next two days while strengthening rapidly. Felicia peaked in intensity at 64 m s^{-1} on 6 August 2009, gradually weakened while bending back toward the west over the next five days, and eventually dissipated east of Hawaii on 11 August 2009.

Figure 9b shows the trajectory of Felicia through ventilation index and normalized intensity phase space. The solid gray line denotes the approximate climatological separation between weakening and strengthening storms, or the equilibrium boundary in Fig. 7a. The shaded regions correspond to where >30% of the TCs in the historical record rapidly strengthen or weaken. The color gradation along Felicia's trajectory is the actual intensity, while the triangles represent the subsequent 24-h normalized intensification. Upward pointing triangles denote strengthening, and the size of the triangle reflects the magnitude of the strengthening. The largest triangles represent the nominal rapid strengthening threshold. Similarly, downward pointing triangles denote weakening.

Felicia developed in an environment of low ventilation and proceeded to intensify rapidly. The hurricane entered the danger zone for rapid intensification and took advantage of the favorable environment to continue to do so. The intensification slowed somewhat as it approached the equilibrium boundary; however, it still overshot its potential intensity. After 6 August 2009, the ventilation began to increase as Felicia entered a less favorable environment characterized by increasing entropy deficit, increasing vertical wind shear, and lower potential intensity. As a result, the TC began to weaken. As the ventilation index continued to increase to large values

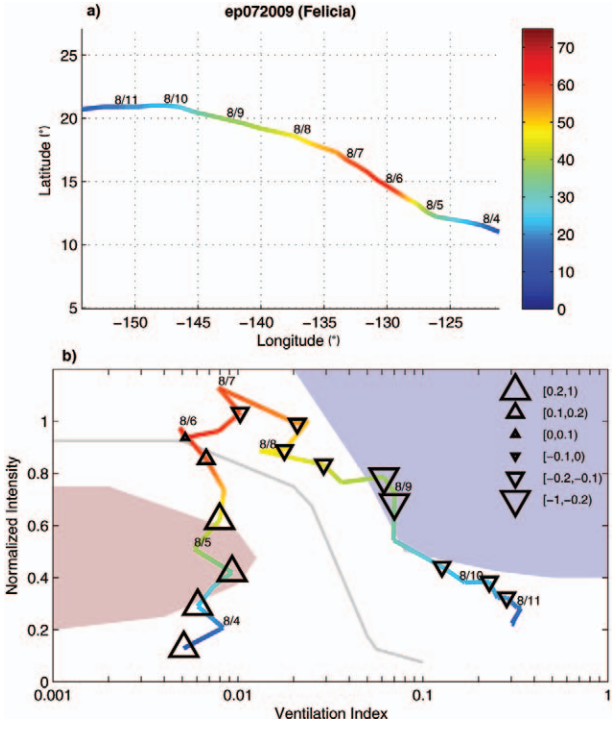

Fig. 9. (a) The track of Hurricane Felicia with the intensity in m s^{-1} given by the color along the track. (b) Hurricane Felicia's trajectory through ventilation index and normalized intensity phase space. Solid gray line denotes the equilibrium boundary from Fig. 7a, and shaded regions denote the rapidly strengthening (light red) and rapidly weakening (light blue) regions from Fig. 8. Color along the trajectory gives the actual intensity. The triangles denote the subsequent 24-h normalized intensification, with upward (downward) pointing triangles reflecting strengthening (weakening). The size of the triangle gives the magnitude of the normalized intensification.

due primarily to increasing vertical wind shear, the weakening rate increased, especially around 9 August 2009 when the weakening was rapid.

Felicia's trajectory through ventilation index and normalized intensity phase space serves as a compact diagnostic to assess changes in intensity due to ventilation. In a real-time setting, forecast trajectories of a similar type can be used as guidance aids and to assess model errors in intensity.

As an example, Fig. 10 shows the 0000 UTC 5 August 2009 ECMWF forecast track and forecast trajectory in ventilation index and normalized intensity phase space. The ECMWF intensity forecast is adjusted by adding a constant equal to the difference between the 0000 UTC 5 August 2009 best-track intensity and the ECMWF analysis intensity.[5] The 5-day forecast track is clearly to the northwest of the actual storm track. Comparing Figs. 9a and 10a, the forecast intensity is also as much as 20 m s^{-1} lower than the verifying intensity.

As shown in Fig. 10b, the ECMWF forecast track error over the first 24 h places Felicia in an environment with higher forecast ventilation indices. The error is due to lower potential intensities and higher midlevel entropy deficits. Over the following day, the forecast wind shear is too high, which causes the ventilation index to continue to be too high. This is consistent with the lower amount of normalized strengthening noted in the ECMWF from 5 to 7 August 2009. The ECMWF does approximately show the same increase in ventilation from 7 to 9 August 2009 compared to the verification, and correspondingly has Felicia halting its steady intensification. In hindsight, the forecast of Felicia is in substantial error in the first few days, and this diagnostic provides useful information as to why this error occurred from a ventilation perspective.

One could repeat this exercise using a multimodel ensemble approach of different numerical weather models or using single model ensembles, provided some intensity bias correction is applied. Caution must be exercised for models of varying resolution due to the ability of higher resolution models to increasingly resolve the warm-core structure of the tropical cyclone, which would affect the entropy deficit. Additionally, it should be kept in mind that ventilation is only one factor responsible for intensity change, as there are a host of environmental and internal mechanisms that make intensity prediction challenging.

With this challenge in mind and for more general TC cases that are not ventilation dominated, a probabilistic approach may be more useful to consider. Given the normalized intensity and analyzed ventilation index, past TCs with similar values of these two quantities can be used to construct a probability distribution function of the climatological 24-h intensity change. As an example, consider the ECMWF analysis for Hurricane Felicia again from 0000 UTC 5 August 2009. Figure 11 shows a histogram of the 24-h intensity change of all historical TCs that fall within 10% of Felicia's bias corrected normalized intensity and ECMWF ventilation index at the analysis time. Note that the 24-h intensity change has been redimensionalized in terms of actual change in wind speed using the 24-h forecast potential intensity from the ECMWF model track forecast.

There is quite a large spread in the 24-h intensity change distribution due to other factors that control

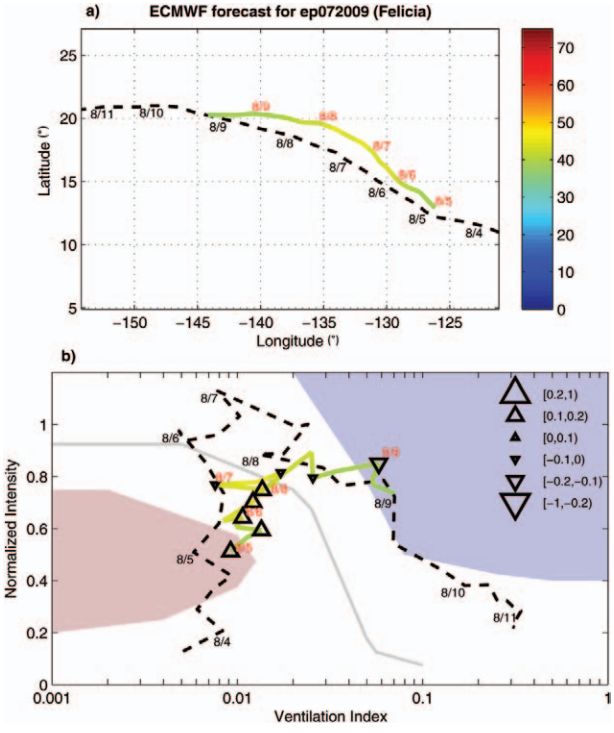

Fig. 10. (a) The forecast track and intensity in m s^{-1} of Hurricane Felicia from the ECMWF model initialized at 0000 UTC 5 Aug 2009. The verifying track is given by the dashed black line. (b) Hurricane Felicia's forecast trajectory through ventilation index and normalized intensity phase space from the ECMWF model. The verifying trajectory is given by the dashed black line.

[5] Global numerical weather prediction models lack the resolution to predict the intensity and inner-core structure of TCs. As such, an adjustment procedure to bias correct the intensity is employed that is identical to that used in the Automated Tropical Cyclone Forecasting system.

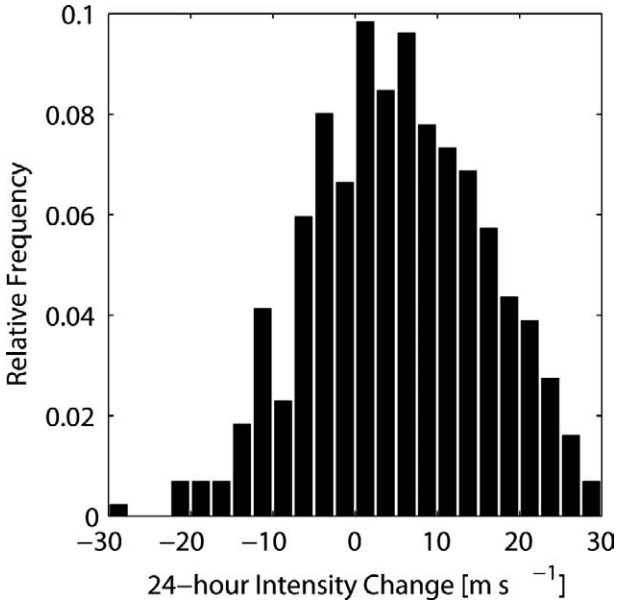

Fig. 11. Normalized histogram of the climatological 24-h intensity change for TCs with similar normalized intensities and ventilation indices as Hurricane Felicia on 0000 UTC 5 Aug 2009, as analyzed by the ECMWF model.

TC intensity. Still, there is clearly a preference toward intensifying storms. From climatology alone, there is a 69% chance that Felicia strengthens and a 31% chance that Felicia weakens in the subsequent 24 h. Furthermore, there is a 19% chance that the intensification is rapid and a 2% chance that the weakening is rapid. Cumulative probabilities and exceedance probabilities can likewise be easily generated. Such probabilities can be used to supplement existing forecasting methods and serve as baseline intensity guidance.

CONCLUSIONS. Vertical wind shear is generally thought to be unfavorable for both tropical cyclogenesis and TC intensification. One hypothesized way vertical wind shear affects TCs is by ventilating the TC with low-entropy air from the environment. Based on an idealized ventilation framework, a ventilation index is derived that equals the environmental vertical wind shear times the nondimensional midlevel entropy deficit divided by the potential intensity. The ventilation index can be calculated from large-scale gridded fields and factors in the dependence on the background thermodynamic state. Both of these qualities make it useful for evaluating whether ventilation plays a detectable role in current TC climatology.

The seasonal distribution of TC genesis points is confined to regions of low seasonal ventilation. Moreover, the ventilation index is able to distinguish environments that are more favorable for developing tropical disturbances compared to nondeveloping tropical disturbances. The vast majority of TCs undergo genesis when the ventilation index is less than 0.1. However, having a ventilation index below this value is not a sufficient condition for genesis (i.e., lower ventilation indices only increase the odds of genesis). In the cases where genesis occurs, there is an average incubation time of two to three days that allows the disturbance to moisten the troposphere.

Ventilation also constrains the normalized intensification of a TC. Intensifying TCs tend to occur at lower values of ventilation compared to weakening TCs. Moreover, there appears to be an equilibrium boundary in ventilation index and normalized intensity phase space toward which TCs tend to strengthen or weaken. To the left of and below the equilibrium boundary, namely TCs at ventilation indices less than 0.03 and normalized intensities less than 0.9, TCs tend to strengthen. The greatest strengthening occurs at ventilation indices less than 0.01 and between normalized intensities of 0.2 and 0.7. To the right of and above the equilibrium boundary, TCs tend to weaken, with the greatest weakening at ventilation indices greater than 0.04 and normalized intensities greater than 0.5. These results generally support the findings of Tang and Emanuel, especially for more intense TCs.

Some examples of operational applications are given by plotting the trajectory of individual storms in ventilation index and normalized intensity phase space to diagnose ventilation-induced changes in intensity in both retrospective and real-time modes. Such a diagnosis works best for storms that are ventilation dominated, as is the case with many east Pacific storms. For other storms, there is generally more variability that makes diagnosing ventilation-induced intensity changes more challenging.

In these more challenging cases, deterministic and probabilistic approaches may be more useful to enhance and supplement existing forecasting methods. The ventilation index can be used as a variable in deterministic statistical intensity models, such as the Statistical Hurricane Intensity Prediction Scheme (SHIPS; DeMaria et al. 2005). Although SHIPS already includes elements of the ventilation index, the nonlinear nature of the ventilation index may suggest an important statistical interaction not considered previously. Additionally, a probabilistic approach based on historical TCs with similar normalized intensities and ventilation indices can be used to assess the probability of weakening and strengthening, along with the probabilities of whether the intensity change will be rapid.

Along with real-time TC forecasting, ventilation diagnostics can serve as a useful tool for assessing model errors over a season or longer. If a model has an intensity or genesis bias, assessing the ventilation index may yield insights in to the causes behind these model biases. For instance, a positive moisture bias at midlevels leads to a ventilation index that is biased low, causing the model to produce too many TCs and/or intensify storms too rapidly. Even small biases in the ventilation index may yield large sensitivities in both the genesis and intensification statistics in a given model.

In conclusion, there are a number of potential uses of the ventilation index that may be of utility to the research and operational tropical cyclone communities.

ACKNOWLEDGMENTS. We thank Dave Nolan, Mark DeMaria, Chris Landsea, Mike Montgomery, John Molinari, Chris Davis, Jonathan Vigh, and an anonymous reviewer for their suggestions that helped improve an earlier version of this manuscript. Buck Sampson and Edward Fukada helped supply the JTWC invest positions. This work was supported by NSF Grant ATM-0850639.

REFERENCES

Bister, M., and K. Emanuel, 1997: The genesis of Hurricane Guillermo: TEXMEX analyses and a modeling study. *Mon. Wea. Rev.,* **125,** 2662–2682.

——, and ——, 2002: Low frequency variability of tropical cyclone potential intensity. 1. Interannual to interdecadal variability. *J. Geophys. Res.,* **107,** 4801, doi:10.1029/2001JD000776.

Bracken, W., and L. Bosart, 2000: The role of synoptic-scale flow during tropical cyclogenesis over the North Atlantic Ocean. *Mon. Wea. Rev.,* **128,** 353–376.

Bryan, G., 2008: On the computation of pseudoadiabatic entropy and equivalent potential temperature. *Mon. Wea. Rev.,* **136,** 5239–5245.

Cram, T., J. Persing, M. Montgomery, and S. Braun, 2007: A Lagrangian trajectory view on transport and mixing processes between the eye, eyewall, and environment using a high-resolution simulation of Hurricane Bonnie (1998). *J. Atmos. Sci.,* **64,** 1835–1856.

Davis, C., and L. Bosart, 2006: The formation of Hurricane Humberto (2001): The importance of extratropical precursors. *Quart. J. Roy. Meteor. Soc.,* **132,** 2055–2085.

Dee, D., and Coauthors, 2011: The ERA-Interim reanalysis: Configuration and performance of the data assimilation system. *Quart. J. Roy. Meteor. Soc.,* **137,** 553–597.

DeMaria, M., 1996: The effect of vertical shear on tropical cyclone intensity change. *J. Atmos. Sci.,* **53,** 2076–2088.

——, 2009: A simplified dynamical system for tropical cyclone intensity prediction. *Mon. Wea. Rev.,* **137,** 68–82.

——, J. Knaff, and B. Connell, 2001: A tropical cyclone genesis parameter for the tropical Atlantic. *Wea. Forecasting,* **16,** 219–233.

——, M. Mainelli, L. Shay, J. Knaff, and J. Kaplan, 2005: Further improvements to the Statistical Hurricane Intensity Prediction Scheme (SHIPS). *Wea. Forecasting,* **20,** 531–543.

Dunkerton, T., M. Montgomery, and Z. Wang, 2009: Tropical cyclogenesis in a tropical wave critical layer: Easterly waves. *Atmos. Chem. Phys.,* **9,** 5587–5646.

Emanuel, K., 1989: The finite-amplitude nature of tropical cyclogenesis. *J. Atmos. Sci.,* **46,** 3431–3456.

——, 2010: Tropical cyclone activity downscaled from NOAA–CIRES reanalysis, 1908–1958. *J. Adv. Model. Earth Syst.,* **2** (1), doi:10.3894/JAMES.2010.2.1.

——, and D. Nolan, 2004: Tropical cyclone activity and the global climate system. Preprints, *26th Conf. on Hurricanes and Tropical Meteorology,* Miami, FL, Amer. Meteor. Soc., 240–241.

——, C. DesAutels, C. Holloway, and R. Korty, 2004: Environmental control of tropical cyclone intensity. *J. Atmos. Sci.,* **61,** 843–858.

Frank, W., and E. Ritchie, 2001: Effects of vertical wind shear on the intensity and structure of numerically simulated hurricanes. *Mon. Wea. Rev.,* **129,** 2249–2269.

Franklin, J., M. Black, and K. Valde, 2003: GPS dropwindsonde wind profiles in hurricanes and their operational implications. *Wea. Forecasting,* **18,** 32–44.

Gallina, G., and C. Velden, 2002: Environmental vertical wind shear and tropical cyclone intensity change utilizing enhanced satellite derived wind information. Preprints, *25th Conf. on Hurricanes and Tropical Meteorology,* San Diego, CA, Amer. Meteor. Soc., 172–173.

Gray, W., 1968: Global view of the origin of tropical disturbances and storms. *Mon. Wea. Rev.,* **96,** 669–700.

——, 1979: Hurricanes: Their formation, structure, and likely role in the tropical circulation. *Meteorology over the Tropical Oceans,* D. B. Shaw, Ed., Royal Meteorological Society, 155–218.

Kaplan, J., and M. DeMaria, 2003: Large-scale characteristics of rapidly intensifying tropical cyclones in the North Atlantic basin. *Wea. Forecasting,* **18,** 1093–1108.

Marin, J., D. Raymond, and G. Raga, 2009: Intensification of tropical cyclones in the GFS model. *Atmos. Chem. Phys.,* **9,** 1407–1417.

McBride, J., and R. Zehr, 1981: Observational analysis of tropical cyclone formation. Part II: Comparison of non-developing versus developing systems. *J. Atmos. Sci.,* **38,** 1132–1151.

Molinari, J., and D. Vollaro, 2010: Rapid intensification of a sheared tropical storm. *Mon. Wea. Rev.,* **138,** 3869–3885.

——, P. Dodge, D. Vollaro, K. Corbosiero, and F. Marks, 2006: Mesoscale aspects of the downshear reformation of a tropical cyclone. *J. Atmos. Sci.,* **63,** 341–354.

Nolan, D., 2007: What is the trigger for tropical cyclogenesis? *Aust. Meteor. Mag.,* **56,** 241–266.

——, and M. Montgomery, 2002: Nonhydrostatic, three-dimensional perturbations to balanced, hurricane-like vortices. Part I: Linearized formulation, stability, and evolution. *J. Atmos. Sci.,* **59,** 2989–3020.

——, and E. Rappin, 2008: Increased sensitivity of tropical cyclogenesis to wind shear in higher SST environments. *Geophys. Res. Lett.,* **35,** L14805, doi:10.1029/2008GL034147.

——, and M. McGauley, 2012: Tropical cyclogenesis in wind shear: Climatological relationships and physical processes. *Cyclones: Formation, Triggers, and Control,* K. Oouchi and H. Fudeyasu, Eds., Nova Science, in press.

Powell, M., 1990: Boundary layer structure and dynamics in outer hurricane rainbands. Part II: Downdraft modification and mixed layer recovery. *Mon. Wea. Rev.,* **118,** 918–938.

Rappaport, E., J. Franklin, A. Schumacher, M. DeMaria, L. Shay, and E. Gibney, 2010: Tropical cyclone intensity change before U.S. Gulf Coast landfall. *Wea. Forecasting,* **25,** 1380–1396.

Rappin, E., D. Nolan, and K. Emanuel, 2010: Thermodynamic control of tropical cyclogenesis in environments of radiative–convective equilibrium with shear. *Quart. J. Roy. Meteor. Soc.,* **136,** 1954–1971.

Raymond, D., and S. Sessions, 2007: Evolution of convection during tropical cyclogenesis. *Geophys. Res. Lett.,* **34,** L06811, doi:10.1029/2006GL028607.

Riemer, M., and M. Montgomery, 2011: Simple kinematic models for the environmental interaction of tropical cyclones in vertical wind shear. *Atmos. Chem. Phys.,* **11,** 9395–9414.

——, ——, and M. Nicholls, 2010: A new paradigm for intensity modification of tropical cyclones: Thermodynamic impact of vertical wind shear on the inflow layer. *Atmos. Chem. Phys.,* **10,** 3163–3188.

Schwerdt, R., F. Ho, and R. Watkins, 1979: Meteorological criteria for standard project hurricane and probable maximum hurricane windfields: Gulf and Atlantic Coasts of the United States. NOAA Tech. Rep. NWS23. 320 pp. [Available online at http://docs.lib.noaa.gov/noaa_documents/NWS/TR_NWS/TR_NWS_23.pdf.]

Simpson, R., and R. Riehl, 1958: Mid-tropospheric ventilation as a constraint on hurricane development and maintenance. Preprints, *Tech. Conf. on Hurricanes,* Miami Beach, FL, Amer. Meteor. Soc., D4-1–D4-10.

Tang, B., and K. Emanuel, 2010: Midlevel ventilation's constraint on tropical cyclone intensity. *J. Atmos. Sci.,* **67,** 1817–1830.

Tory, K., N. Davidson, and M. Montgomery, 2007: Prediction and diagnosis of tropical cyclone formation in an NWP system. Part III: Diagnosis of developing and nondeveloping storms. *J. Atmos. Sci.,* **64,** 3195–3213.

Wong, M., and J. Chan, 2004: Tropical cyclone intensity in vertical wind shear. *J. Atmos. Sci.,* **61,** 1859–1876.

Wu, L., and S. Braun, 2004: Effects of environmentally induced asymmetries on hurricane intensity: A numerical study. *J. Atmos. Sci.,* **61,** 3065–3081.

Zehr, R., 1992: Tropical cyclogenesis in the western north Pacific. NOAA Tech. Rep. NESDIS 61, 181 pp.